Published in final edited form as:
J Biomed Mater Res A. 2011 June 15; 97(4): 414–422. doi:10.1002/jbm.a.33062.

Human dental pulp progenitor cell behavior on aqueous and hexafluoroisopropanol (HFIP) based silk scaffolds

Weibo Zhang[1], **Ivy Pruitt Ahluwalia**[1], **Robert Literman**[1,*], **David L. Kaplan**[2], and **Pamela C. Yelick**[1]

[1] Division of Craniofacial and Molecular Genetics, Department of Oral and Maxillofacial Pathology, Tufts University School of Dental Medicine, Boston, Massachusetts

[2] Department of Biomedical Engineering, Tufts University, Medford, Massachusetts

Abstract

Silk scaffolds have been successfully used for a variety of tissue engineering applications due to their biocompatibility, diverse physical characteristics, and ability to support cell attachment and proliferation. Our prior characterization of 4-day postnatal rat tooth bud cells grown on hexafluoro-2-propanol (HFIP) silk scaffolds showed that the silk scaffolds not only supported osteodentin formation, but also guided the size and shape of the formed osteodentin. In this study, interactions between human dental pulp cells and HFIP and aqueous based silk scaffolds were studied under both *in vitro* and *in vivo* conditions. Silk scaffold porosity and incorporation of RGD and DMP peptides were examined. We found that the degradation of aqueous based silk is much faster than HFIP based silk scaffolds. Also, HFIP based silk scaffolds supported the soft dental pulp formation better than the aqueous based silk scaffolds. No distinct hard tissue regeneration was found in any of the implants, with or without additional cells. We conclude that alternative silk scaffold materials, and hDSC pre-seeding cell treatments or sorting and enrichment methods, need to be considered for successful dental hard tissue regeneration.

Keywords

Silk scaffolds; dental pulp cells; dental tissue regeneration; degradation

INTRODUCTION

Studies on tooth regeneration have been performed for decades, and numerous approaches have been investigated. However, it remains uncertain which methods will be most useful for dental tissue regeneration. Promising results include the formation of dentin-like tissue in implants consisting of dental pulp stem cells (DPSCs) and hydroxyapatite/tricalcium phosphate (HA/TCP) powder as a carrier vehicle[1,2]. Comparison of DPSCs grown on three types of 3-dimentional (3D) scaffolds - HA/TCP, Titanium, and collagen – revealed that limited amounts of hard tissue were detected only in the HA/TCP implants, and not in the two other types of implants[3]. Another promising approach reported the formation of recognizable tooth structures, containing organized enamel, dentin, and a well-defined tooth pulp, in constructs containing Polyglycolate/poly-L-lactate (PGA/PLLA) or poly-L-lactate-co-glycolate (PLGA) scaffolds seeded with dissociated postnatal rat and pig tooth bud derived dental epithelial (DE) and dental mesenchymal (DM) cells[4–6]. Similar results were

Corresponding author: Pamela C. Yelick, Department of Oral and Maxillofacial Pathology, Tufts University, 136 Harrison Avenue, Room M824, Boston, MA 02111, Phone: 617-636-2430, Fax: 617-636-2432, pamela.yelick@tufts.edu.
*Currently is a PhD candidate of Department of Ecology, Evolution, and Organismal Biology, Iowa State University, Ames, Iowa

also achieved using DE and DM cells seeded in Collagen sponge constructs[7], where well organized, but very small tooth-like structures were formed. Currently, we are working on approaches that support the regeneration of dental tissues and whole teeth of specified size and shape. This report continues our characterization of scaffolds for dental tissue engineering applications, using scaffolds fabricated by silk fibroin (SF) extracted from silk produced by the *Bombyx mori (B mori)* silkworm, which has been studied in cell culture and tissue engineering for more than 10 years[8]. SF contains alanine and glycine amino acid repeat structures that readily form the β-sheet crystals responsible for the remarkable strength and toughness of SF[9]. SF is also biocompatible, biodegradable and non-toxic[10], and has been shown to support the attachment, proliferation and differentiation of many cell types. For these reasons, SF from *B.mori* silkworm is commonly used for the regeneration of different tissues, including bone[11,12], cartilage[13,14], ligament[15,16], kidney[17], fat[18], and vascular[19].

In a previous publication, we seeded postnatal rat tooth bud cells onto 550 and 250 μm pore sized HFIP silk scaffolds, with and without incorporated Arginine-Glycine-Aspartic acid (RGD) peptide. After 20 weeks of *in vivo* growth in the rat omentum, mineralized osteodentin-like tissues were observed, and in particular, significantly more robust mineralized tissues were found in silk scaffolds of larger pore size (550 versus 250 micron diameter), and containing the RGD peptide. Our results also revealed that the size and shape of the pore guided osteodentin formation, suggesting possible means to manipulate the size and shape of bioengineered mineralized tissues[20]. No dental epithelial cells or enamel were detected in any of these implanted constructs, despite that fact that both rat dental epithelial and mesenchymal cells were used in the study, suggesting that silk may not be a desirable material for enamel cell growth and differentiation under the conditions used in the study. Based on our previous results, here we report results of the influence of silk scaffolds of even larger pore size (1000 μm) on bioengineered tissue formation by adult human dental pulp cells (hDPSCs).

MATERIALS AND METHODS

Cell isolation

Human adult dental pulp cells (DPSCs) harvested from a 3rd molar tooth of a de-identified 16-year old African American female were used in this study. Briefly, the tooth was extracted by a trained clinician at the Tufts School of Dental Medicine, as recommended, following approved protocols. The extracted tooth was split in half using a vice, and the dental pulp was carefully removed from the dental chamber. The isolated dental pulp was minced and digested using 0.3 mg/mL collagenase type I and 0.4 mg/mL dispase, and single cell suspensions were obtained by filtration using a 40 μm cell sieve. Isolated DPCs were cultured in dental pulp medium (DMEM/F12 with 10% FBS, 1% GlutaMAX, 50 μg/ml ascorbic acid, and 1% penicillin/streptomycin/amphotericin (PSA), expanded to passage 3 (P3), and cryopreserved until use.

Bone aspirate from an 18 year old African American male was purchased from Poietics Cell Systems of Lonza Walkersville Inc. (Walkersville, MD). Bone marrow cells (BMCs) were separated by centrifugation, and expanded in DMEM supplemented with 10% FBS, 1% Non essential amino-acids, 1 ng/mL bFGF, and 1% penicillin/streptomycin, and cryopreserved until use.

Silk scaffold preparation

The silk scaffolds were fabricated using fibroin extracted from *B. mori* silkworm cocoons in 0.02-M Na_2CO_3, dissolved in a 9.3-M LiBr solution, and dialyzed using distilled water. Silk

scaffolds with average pores sized 500 μm or 1000 μm were fabricated either by the hexafluoro-2-propanol (HFIP) or aqueous process. For HFIP based silk scaffolds, the silk fibroin aqueous solution was freeze-dried and dissolved in HFIP (17%). For aqueous silk scaffolds, 6% silk fibroin solution was used to generate silk scaffolds with 500 μm pore sizes, and 8% silk fibroin solution was used to fabricate silk scaffolds with 1000 μm pore sizes. Granular NaCl particles either 500–600 μm, or 1000–1180 μm in diameter, were then added to the appropriately prepared water and HFIP based silk fibroin solutions in Teflon cylinder containers.

The salts were leeched out of the scaffolds by immersion in water. Next, RGD peptide, [H]-Gly-Arg-Gly-Asp-Ser-[OH] or dentin matrix protein-1 (DMP-1) peptide, [H]-Gln-Glu-Ser-Gln-Ser-Glu-Gln-Asp-Ser-[OH] was incorporated onto the scaffolds by soaking the scaffolds for 3 hours in 1 mg/mL peptide solution. In summary, eight different silk scaffolds were fabricated: 1–2) HFIP fabricated, 500 μm and 1000 pore sized silk scaffold with RGD; 3–4) aqueous fabricated, 500 and 1000 μm pore sized silk scaffolds with RGD; 5–6) HFIP fabricated, 500 and 1000 μm pore sized silk scaffold coupled with DMP-1 peptide; 7–8) aqueous fabricated 500 and 1000 mm pore sized silk scaffolds coupled with DMP-1 peptide. Fabricated silk scaffolds were cut to standard size (5mm × 3mm × 3mm), sanitized in 70% ethanol overnight, washed with phosphate buffered saline (PBS), and soaked in DMEM medium overnight until use.

In vitro evaluation of human DPSCs and BMSCs on silk scaffolds

Human DPCs and BMCs were seeded onto sterilized HFIP and aqueous based 1000 μm RGD silk scaffolds as follows. For each scaffold, 4.5×10^5 cells were mixed with 100 μl Collagen I (Cat No. 354249, BD biosciences, Bedford, MA) and evenly distributed onto suction-dried scaffolds, using a 200 μl pipette. The cell-seeded scaffolds were incubated at 37°C for 1 hour, and cultured in osteogenic medium (DMEM/10% FBS/1% Non essential amino-acids/100 nM Dexamethasone/10 mM beta Glycerol phosphate/0.05 mM Ascorbic acid/1% Pen-Strep) supplemented with 1μg/ml Calcein (C0875, Sigma, St. Louis, MO). Two types of negative control samples were used in this study, 1) scaffolds alone without cells cultured in the osteogenic medium with Calcein, and 2) cell-seeded scaffolds cultured in the osteogenic medium without Calcein. At weekly intervals, Calcein incorporation and fluorescence was measured using a SpectraMax® M2/M2e Microplate Reader (Molecular, Sunnyvale, CA) with well-scanning set to measure 9 areas per well. For each condition, six samples were assessed. Fluorescent images were documented using a Zeiss Axiophot (Stuttgart, Germany) digital camera at 1 day, 3 weeks and 6 weeks of culture.

In vivo implantation

All animal experiments were performed under the guidance and approval of the Institutional Animal Care and Use Committee (IACUC) of Tufts University. NIH guidelines for the care and use of laboratory animals (NIH Publication #85-23 Rev. 1985) have been observed. Human DPCs were cultured in pulp medium with osteogenic supplements (100 nM Dexamethasone, 10 mM beta glycerol phosphate, and 50 μg/ml Ascorbic acid) for 10 days, and seeded onto scaffolds as described for the *in vitro* study, and cultured overnight before transplantation. Experimental and control replicate samples were transplanted subcutaneously into four week old nude rat hosts (NIH-Foxn1, Charles River, Wilmington, MA), and collected after 6, 18, and 25 weeks. All of the eight different types of fabricated silk scaffold were evaluated *in vivo* study, with 3 experimental and 2 control samples collected at each of the above three developmental times.

Histological analyses of harvested silk scaffold implants

Harvested experimental and control constructs were fixed, embedded in paraffin, and sectioned. For histological evaluation, sections were stained with Hematoxylin and Eosin (H&E) staining. Silk degradation and blood vessel formation were evaluated on the samples collected at 6 weeks. The degradation of HFIP based silk scaffolds was measured as previously described, based on our ability to image HFIP based silk material using a polarized light filter[20]. Water- based silk implants were imaged using normal bright field microscopy. For each implant, four cross-sections were selected and analyzed, and blood vessel formation was evaluated on two center sections. In order to evaluate the entire area of each section, four 100X digital images of each were evaluated for blood vessels greater than 10 μm in diameter.

Statistical analysis

Data were analyzed with statistically significant values defined as $p<0.05$ based on one-way analysis of variance (ANOVA).

RESULTS

Cell isolation and silk scaffold preparation

After cryopreservation, both human DPCs and BMCs retained their typical mesenchymal spindle shaped cell morphology with elongated cell body (Fig. 1). Under bright field microscopy, no significant differences were detectable between HFIP and aqueous based silk scaffolds, or between the scaffolds incorporated with RGD or DMP-1. Pore size difference was easily detected (Fig. 2).

In vitro evaluation

Although no scaffolds appeared fluorescent after 1 day, after three weeks of in vitro culture, distinct Calcein containing calcified nodules were found in all hDPSC and hBMSC cell-seeded samples, with corresponding and strong fluorescence (Fig. 3). No fluorescent signal was detected in scaffolds cultured in Calcein-free media, while fluorescent signals were detected in Calcein cultured non-cell-seeded HFIP and aqueous based silk scaffolds after 6 weeks *in vitro* culture (Fig. 4). Although the fluorescent Calcein signal appeared to increase over time in cell-seeded scaffolds, for reasons that are not clear, no detectable increase was indicated from the spectrophotometer readout data (data not shown).

In vivo implantation

None of the host animals showed any unfavorable reaction to the implants. Implants were clearly noticeable under skin after six weeks implantation (Fig. 5A). After 18 weeks, only HFIP based implants were readily observed (Fig. 5B), and after 25 weeks of subcutaneous transplantation, none of the silk scaffold implant sites were detectable under the skin (Fig. 5C), despite the fact that harvested HFIP based silk scaffolds appeared to retain their basic size and shape after 25 weeks in vivo culture (Fig. 5D). It was very difficult to locate the aqueous silk scaffolds during sample collection (Fig. 5D). It was surprising to find that no calcified tissues were found in any of the experimental cell-seeded or control non-cell-seeded implants after 6 weeks of in vivo culture. In contrast, clear differences in the degradation characteristics of HFIP and aqueous based silk scaffolds were observed. No obvious degradation was detected in HFIP based silk scaffolds, and most of the scaffold pores retained their original size and shape, and contained ingrown tissues. Significant tissue ingrowth was also observed in aqueous based silk scaffolds, although cell-seeded and non-cell-seeded water-based scaffolds exhibited significant degradation over time, as the degraded silk fragments appeared to lose their sharp edges and became round and smooth.

The aqueous based silk implants were also filled with newly formed fibrous tissues, but most pores appeared to be collapsed. Comparatively, after 6 weeks, the remaining volume of aqueous based silk implants appeared to be approximately half that of HFIP based silk implants (Fig. 6). Statistical analysis confirmed that the HFIP based silk scaffolds degraded more slowly than aqueous based silk scaffolds, with or without seeded cells ($P<0.05$). No significant differences were found between cell-seeded and non-cell-seeded scaffolds ($P>0.05$) (Tab. 1). Blood vessel formation quantification also revealed no significant difference between cell seeded aqueous and HFIP based silk implants ($P>0.05$), or between cell-seeded and non-cell- seeded HFIP- or aqueous- based silk implants ($P>0.05$) as shown in Table 2. Although degradation of both water and HFIP based scaffold in vivo implants was observed after 18 weeks, significant degradation was only observed in the HFIP based implants after 25 weeks. At 18 weeks, no noticeable difference was observed between cell-seeded and non-cell-seeded HFIP implants. Polarized light microcopy revealed increased formation of organized collagen in HFIP based as compared to aqueous based implants (Fig. 7).

DISCUSSION

It is well recognized that the proper selection of scaffolding material is essential to support the attachment, proliferation, and differentiation of seeded cells, and to provide easy manipulation for various tissue engineering applications. Scaffold porosity is required to allow efficient cell migration throughout the scaffold, and to guide cell attachment, proliferation, and spreading[21]. Pore size also plays an important role in scaffold degradation rate, which also influences bioengineered and host tissue ingrowth. Scaffolds with prohibitively small pore size achieve only limited cell migration and diffusion of nutrients, but offer larger surface area for cell attachment. Scaffolds containing larger sized pores may degrade faster, and may in turn benefit cell and tissue diffusion, at the expense of surface area for optimal cell adhesion. Optimal pore size for various tissue engineering applications is still under debate due to multiple conflicting reports[22], and similarly, optimized pore size for dental tissue regeneration has not yet been determined. Our previous published results using rat postnatal dental stem cells indicated that increased mineralized osteodentin formation occurred in silk scaffolds with larger pore size (550 versus 250 μm diameter), and furthermore, that larger pores appeared to guide the size and shape of bioengineered osteodentin[20]. In contrast, the results shown here using human dental mesenchymal stem cells, which compared, silk scaffolds with 500 μm and 1000 μm diameter pores, demonstrated that although the scaffold pores appeared to support the formation of soft tissue, no hard tissue was detected in any of the silk implants. In addition, no statistical differences in silk scaffold degradation or blood vessel formation after 6 weeks of in vivo growth were detectable between silk scaffolds of 550 versus 1000 μm pore size diameter.

Published reports indicate that 3D porous silk scaffolds prepared from HFIP are commonly used for bone regeneration[23,24]. HFIP silk scaffolds are suitable for bone regeneration, since the degradation rate of HFIP based silk is very slow, and therefore provides mechanical stability and support for the bone defect site until new bone formation can occur. More recently, aqueous-based silk scaffold fabrication preparation methods were developed, providing scaffolds with similar morphology to the HFIP based silk scaffolds, but with significantly faster degradation rates[25]. Furthermore, aqueous based silk scaffold preparation results in scaffolds that are more biocompatible and have been shown to provide enhanced osteogenic differentiation as compared to the HFIP derived scaffolds[26]. In addition to the facts that aqueous based silk scaffolds are significantly more susceptible to proteolytic hydrolysis and biocompatibility, they also appear to facilitate early stages of new bone formation.

In agreement, our results shown here also demonstrate that aqueous-based fabricated silk scaffolds degraded much faster than the HFIP based silk scaffolds. Because of the high degradation rate of aqueous-based silk scaffolds, the tissue surrounding the degrading scaffold appeared to be newly formed, and therefore less mature. The use of silk protein based materials for human applications has gained FDA approval, and has extensively been used for both hard and soft tissue engineering applications[27]. In addition to providing suitable biocompatibility, silk fibroin proteins can be modified by carbodiimide coupling to allow for the conjugation of additional molecules, such as growth factors[26,28], to benefit bioengineered tissue formation. RGD is a cell attachment peptide which is generally found in some naturally formed silk but not in the domesticated silk[8]. RGD peptides can enhance cell adhesion to biomaterials via integrin receptors, and thereby stimulate new tissue formation[29]. Our previous publication showed that RGD peptide improved mineralized tissue formation on silk based scaffolds[20]. To expand our earlier studies, here we also examined the utility of DMP-1 containing silk scaffolds, based on the fact that this acidic and phosphorylated extracellular matrix protein is expressed in odontoblast, predentin, and dentin[30], and that loss of DMP-1 results in dentin anomalies, including partial failure of predentin maturation into dentin, and hypomineralization[31]. Enhanced osteo-integration was also observed in DMP-1 pre-treated implants[32]. In this study, we compared mineralized tissue formation by hDPSCs in RGD or DMP-1 incorporated silk scaffolds. Surprisingly, no hard tissue formation was observed in either RGD or DMP-1 peptide containing silk scaffolds. In addition, no significant different soft tissue formation was detected between silk scaffolds with or without additional RGD or DMP-1 peptide motif.

We anticipate that appropriate interactions between the scaffold material and cells are essential for tissue-specific regeneration. We have previously demonstrated that HFIP based silk scaffolds can support osteodentin formation when seeded with primary cultures of 4dpn rat tooth bud cells. However, for practical applications, it must be recognized that it is difficult, if not impossible, to obtain early post-natal human tooth bud tissues for autologous dental tissue regeneration in adults. The fact that stem cells have been isolated and characterized from human postnatal dental tissues including dental pulp[33-35], periodontal ligament[36,37], and periapical follicle[38], indicates that adult dental tissues may offer useful cell sources for DSCs for dental tissue regeneration. An additional consideration is that cryopreservation is necessary to preserve DSCs if suitable DSC banks are envisioned for clinical applications for dental tissue engineering.

Surprisingly, in this study, no hard tissue formation was observed in any of the eight different silk scaffold fabrications tested, despite that fact that significant calcified nodule formation was observed in *in vitro* cultured DSC-silk scaffold constructs. Our results correlate well with other published reports[3,39], which suggest that *in vitro* calcification is not a sufficient indicator for *in vivo* conditions. Furthermore, immunohistochemical analysis by human anti-human mitochondria antibody showed limited amount of positive cells remaining in the implant even after 6 weeks transplantation. Our results highlight the need for alternative human dental cell enrichment and scaffold selection, and also cell priming and pre-treatment methods.

In contrast to our anticipation that silk scaffolds would exhibit utility in mineralized tissue formation by human dental pulp derived cells, the results of this study suggest that silk scaffolds seeded with human DSPs may be useful for soft tissue, dental pulp regeneration. Dental pulp regeneration requires scaffold materials that can reliably support the vascularization and innervations of pulp tissue. Although we did not observe any significant difference in blood vessel formation between HFIP and aqueous based fabricated silk scaffolds, we did observe that soft tissue formation in aqueous based silk scaffolds appeared less organized and that newly formed collagen-containing ECM appeared less mature, and

less organized, as compared to that of HFIP-based scaffolds. We conclude that HFIP based silk scaffolds may provide a more suitable environment for soft dental pulp tissue generation by adult DPSCs.

Calcein fluorescent staining has been widely used to indicate the live formation of calcified nodules[40,41]. In this study, Calcein staining can clearly indicate mineralized nodule formation. However, our readout of fluorescent signal under 3-D conditions is not correlated with the actual signals. A reliable method needs to be developed to solve this problem.

CONCLUSIONS

In this study, we systematically investigated the *in vitro* and *in vivo* response of human dental pulp cells to three-dimensional HFIP and aqueous based SF silk porous scaffolds of varying average pore size, 500 and 1000 um diameter, with either RGD or DMP-1 peptide protein modification. Our results demonstrated that all silk scaffolds were well tolerated by host animals, whether they were cell-seeded or not. In addition, we found that although neither scaffold type supported osteodentin formation as expected, HFIP based silk scaffolds appeared to support soft tissue dental pulp formation better than the corresponding aqueous based silk scaffolds. The lack of mineralized tissue formation in any of the *in vivo* implanted cell-scaffold implants was surprising, based on our earlier published results, and despite the fact that distinct calcified nodule formation was observed in *in vitro* cultured cell-scaffold constructs. These results emphasize the fact that additional studies are required to determine whether specific cell pretreatment protocols, or additional cell sorting methods, can be used to facilitate both hard and soft tissue formation by hDPCS, for future dental tissue regeneration applications.

Acknowledgments

We would like to acknowledge input from all Yelick and Kaplan Laboratory members, and support from NIH/NIDCR R01 DE016132 (PCY) and NIH R01 EB003210 and P41 EB002520 (DK).

References

1. Gronthos S, Brahim J, Li W, Fisher LW, Cherman N, Boyde A, DenBesten P, Robey PG, Shi S. Stem cell properties of human dental pulp stem cells. J Dent Res. 2002; 81(8):531–5. [PubMed: 12147742]
2. Mao JJ, Giannobile WV, Helms JA, Hollister SJ, Krebsbach PH, Longaker MT, Shi S. Craniofacial tissue engineering by stem cells. J Dent Res. 2006; 85(11):966–79. [PubMed: 17062735]
3. Zhang W, Walboomers XF, van Kuppevelt TH, Daamen WF, Bian Z, Jansen JA. The performance of human dental pulp stem cells on different three-dimensional scaffold materials. Biomaterials. 2006; 27(33):5658–68. [PubMed: 16916542]
4. Young CS, Terada S, Vacanti JP, Honda M, Bartlett JD, Yelick PC. Tissue engineering of complex tooth structures on biodegradable polymer scaffolds. J Dent Res. 2002; 81(10):695–700. [PubMed: 12351668]
5. Duailibi MT, Duailibi SE, Young CS, Bartlett JD, Vacanti JP, Yelick PC. Bioengineered teeth from cultured rat tooth bud cells. J Dent Res. 2004; 83(7):523–8. [PubMed: 15218040]
6. Young CS, Abukawa H, Asrican R, Ravens M, Troulis MJ, Kaban LB, Vacanti JP, Yelick PC. Tissue-engineered hybrid tooth and bone. Tissue Eng. 2005; 11(9-10):1599–610. [PubMed: 16259613]
7. Sumita Y, Honda MJ, Ohara T, Tsuchiya S, Sagara H, Kagami H, Ueda M. Performance of collagen sponge as a 3-D scaffold for tooth-tissue engineering. Biomaterials. 2006; 27(17):3238–48. [PubMed: 16504285]
8. Wang Y, Kim HJ, Vunjak-Novakovic G, Kaplan DL. Stem cell-based tissue engineering with silk biomaterials. Biomaterials. 2006; 27(36):6064–82. [PubMed: 16890988]

9. Cao Y, Wang B. Biodegradation of silk biomaterials. Int J Mol Sci. 2009; 10(4):1514–24. [PubMed: 19468322]
10. Meinel L, Hofmann S, Karageorgiou V, Kirker-Head C, McCool J, Gronowicz G, Zichner L, Langer R, Vunjak-Novakovic G, Kaplan DL. The inflammatory responses to silk films in vitro and in vivo. Biomaterials. 2005; 26(2):147–55. [PubMed: 15207461]
11. Jones GL, Motta A, Marshall MJ, El Haj AJ, Cartmell SH. Osteoblast: osteoclast co-cultures on silk fibroin, chitosan and PLLA films. Biomaterials. 2009; 30(29):5376–84. [PubMed: 19647869]
12. Meinel L, Fajardo R, Hofmann S, Langer R, Chen J, Snyder B, Vunjak-Novakovic G, Kaplan D. Silk implants for the healing of critical size bone defects. Bone. 2005; 37(5):688–98. [PubMed: 16140599]
13. Hofmann S, Knecht S, Langer R, Kaplan DL, Vunjak-Novakovic G, Merkle HP, Meinel L. Cartilage-like tissue engineering using silk scaffolds and mesenchymal stem cells. Tissue Eng. 2006; 12(10):2729–38. [PubMed: 17518642]
14. Wang Y, Kim UJ, Blasioli DJ, Kim HJ, Kaplan DL. In vitro cartilage tissue engineering with 3D porous aqueous-derived silk scaffolds and mesenchymal stem cells. Biomaterials. 2005; 26(34): 7082–94. [PubMed: 15985292]
15. Fan H, Liu H, Wang Y, Toh SL, Goh JC. Development of a silk cable-reinforced gelatin/silk fibroin hybrid scaffold for ligament tissue engineering. Cell Transplant. 2008; 17(12):1389–401. [PubMed: 19364076]
16. Moreau JE, Chen J, Horan RL, Kaplan DL, Altman GH. Sequential growth factor application in bone marrow stromal cell ligament engineering. Tissue Eng. 2005; 11(11-12):1887–97. [PubMed: 16411835]
17. Subramanian B, Rudym D, Cannizzaro C, Perrone R, Zhou J, Kaplan DL. Tissue-Engineered Three-Dimensional In Vitro Models for Normal and Diseased Kidney. Tissue Eng Part A.
18. Mauney JR, Nguyen T, Gillen K, Kirker-Head C, Gimble JM, Kaplan DL. Engineering adipose-like tissue in vitro and in vivo utilizing human bone marrow and adipose-derived mesenchymal stem cells with silk fibroin 3D scaffolds. Biomaterials. 2007; 28(35):5280–90. [PubMed: 17765303]
19. Zhang X, Baughman CB, Kaplan DL. In vitro evaluation of electrospun silk fibroin scaffolds for vascular cell growth. Biomaterials. 2008; 29(14):2217–27. [PubMed: 18279952]
20. Xu WP, Zhang W, Asrican R, Kim HJ, Kaplan DL, Yelick PC. Accurately shaped tooth bud cell-derived mineralized tissue formation on silk scaffolds. Tissue Eng Part A. 2008; 14(4):549–57. [PubMed: 18352829]
21. Tai H, Mather ML, Howard D, Wang W, White LJ, Crowe JA, Morgan SP, Chandra A, Williams DJ, Howdle SM, et al. Control of pore size and structure of tissue engineering scaffolds produced by supercritical fluid processing. Eur Cell Mater. 2007; 14:64–77. [PubMed: 18085505]
22. Murphy CM, Haugh MG, O'Brien FJ. The effect of mean pore size on cell attachment, proliferation and migration in collagen-glycosaminoglycan scaffolds for bone tissue engineering. Biomaterials. 31(3):461–6. [PubMed: 19819008]
23. Park SY, Ki CS, Park YH, Jung HM, Woo KM, Kim HJ. Electrospun silk fibroin scaffolds with macropores for bone regeneration: an in vitro and in vivo study. Tissue Eng Part A. 16(4):1271–9. [PubMed: 19905876]
24. Jiang X, Zhao J, Wang S, Sun X, Zhang X, Chen J, Kaplan DL, Zhang Z. Mandibular repair in rats with premineralized silk scaffolds and BMP-2-modified bMSCs. Biomaterials. 2009; 30(27): 4522–32. [PubMed: 19501905]
25. Kim UJ, Park J, Kim HJ, Wada M, Kaplan DL. Three-dimensional aqueous-derived biomaterial scaffolds from silk fibroin. Biomaterials. 2005; 26(15):2775–85. [PubMed: 15585282]
26. Kim HJ, Kim UJ, Vunjak-Novakovic G, Min BH, Kaplan DL. Influence of macroporous protein scaffolds on bone tissue engineering from bone marrow stem cells. Biomaterials. 2005; 26(21): 4442–52. [PubMed: 15701373]
27. Altman GH, Diaz F, Jakuba C, Calabro T, Horan RL, Chen J, Lu H, Richmond J, Kaplan DL. Silk-based biomaterials. Biomaterials. 2003; 24(3):401–16. [PubMed: 12423595]

28. Jin HJ, Chen J, Karageorgiou V, Altman GH, Kaplan DL. Human bone marrow stromal cell responses on electrospun silk fibroin mats. Biomaterials. 2004; 25(6):1039–47. [PubMed: 14615169]
29. Hersel U, Dahmen C, Kessler H. RGD modified polymers: biomaterials for stimulated cell adhesion and beyond. Biomaterials. 2003; 24(24):4385–415. [PubMed: 12922151]
30. Aguiar MC, Arana-Chavez VE. Immunocytochemical detection of dentine matrix protein 1 in experimentally induced reactionary and reparative dentine in rat incisors. Arch Oral Biol. 55(3): 210–4. [PubMed: 20138611]
31. Ye L, MacDougall M, Zhang S, Xie Y, Zhang J, Li Z, Lu Y, Mishina Y, Feng JQ. Deletion of dentin matrix protein-1 leads to a partial failure of maturation of predentin into dentin, hypomineralization, and expanded cavities of pulp and root canal during postnatal tooth development. J Biol Chem. 2004; 279(18):19141–8. [PubMed: 14966118]
32. Hassan AH, Evans CA, Zaki AM, George A. Use of bone morphogenetic protein-2 and dentin matrix protein-1 to enhance the osteointegration of the Onplant system. Connect Tissue Res. 2003; 44(1):30–41. [PubMed: 12945802]
33. Gronthos S, Mankani M, Brahim J, Robey PG, Shi S. Postnatal human dental pulp stem cells (DPSCs) in vitro and in vivo. Proc Natl Acad Sci U S A. 2000; 97(25):13625–30. [PubMed: 11087820]
34. Zhang W, Walboomers XF, Shi S, Fan M, Jansen JA. Multilineage differentiation potential of stem cells derived from human dental pulp after cryopreservation. Tissue Eng. 2006; 12(10):2813–23. [PubMed: 17518650]
35. Nakashima M, Iohara K, Sugiyama M. Human dental pulp stem cells with highly angiogenic and neurogenic potential for possible use in pulp regeneration. Cytokine Growth Factor Rev. 2009; 20(5-6):435–40. [PubMed: 19896887]
36. Ivanovski S, Gronthos S, Shi S, Bartold PM. Stem cells in the periodontal ligament. Oral Dis. 2006; 12(4):358–63. [PubMed: 16792719]
37. Silverio KG, Benatti BB, Casati MZ, Sallum EA, Nociti FH Jr. Stem cells: potential therapeutics for periodontal regeneration. Stem Cell Rev. 2008; 4(1):13–9. [PubMed: 18278569]
38. Huang GT, Sonoyama W, Liu Y, Liu H, Wang S, Shi S. The hidden treasure in apical papilla: the potential role in pulp/dentin regeneration and bioroot engineering. J Endod. 2008; 34(6):645–51. [PubMed: 18498881]
39. Zhang W, Walboomers XF, van Osch GJ, van den Dolder J, Jansen JA. Hard tissue formation in a porous HA/TCP ceramic scaffold loaded with stromal cells derived from dental pulp and bone marrow. Tissue Eng Part A. 2008; 14(2):285–94. [PubMed: 18333781]
40. Uchimura E, Machida H, Kotobuki N, Kihara T, Kitamura S, Ikeuchi M, Hirose M, Miyake J, Ohgushi H. In-situ visualization and quantification of mineralization of cultured osteogenetic cells. Calcif Tissue Int. 2003; 73(6):575–83. [PubMed: 12958691]
41. Hayashi O, Katsube Y, Hirose M, Ohgushi H, Ito H. Comparison of osteogenic ability of rat mesenchymal stem cells from bone marrow, periosteum, and adipose tissue. Calcif Tissue Int. 2008; 82(3):238–47. [PubMed: 18305886]

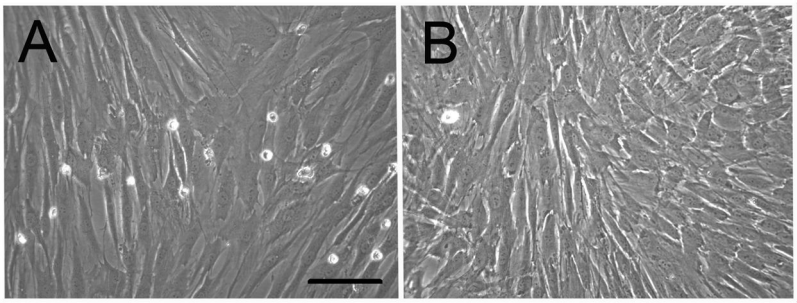

Figure 1. In vitro characterization of human DPSCs and BMSCs

A) Human dental pulp cells (DPSCs). B) Human bone marrow cells (BMSCs). Both types of cells showed typical mesenchymal cells morphology. (Scale bar=200 μm).

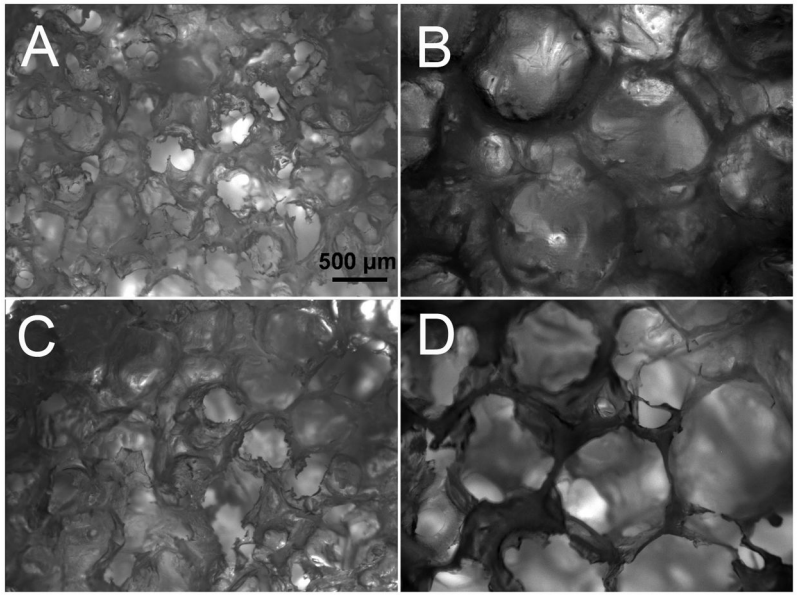

Figure 2. Characterization of HFIP and water based RGD and DMP-1 incorporated silk scaffolds

A) HFIPfabricated, 500 μm pore sized silk scaffold coupled with RGD. B) HFIP fabricated, 1000 μm pore sized silk scaffold coupled with RGD. C) Aqueous-fabricated, 500 μm pore sized silk scaffold coupled with RGD. D) Aqueous fabricated, 1000 μm pore sized silk scaffold coupled with RGD. Scale bar=500 μm. The scaffolds incorporated with DMP-1 peptide showed similar morphology as the scaffolds with RGD.

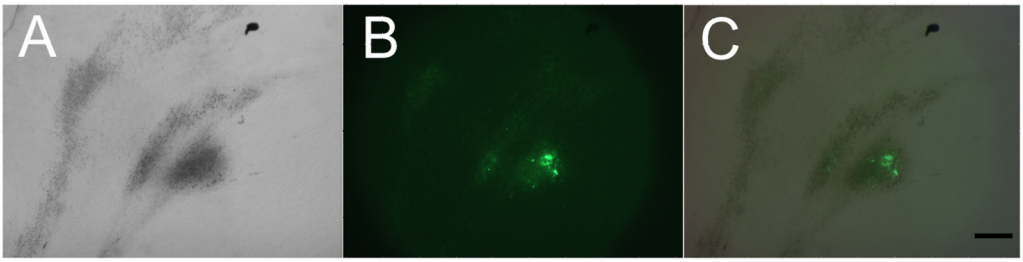

Figure 3. Mineralized tissue formation in 3 week in vitro cultured, calcein containing silk constructs

Calcified nodules formation using (A) bright field, and (B) fluorescent filter. (C) Merged A and B images. (Scale bar = 500 μm).

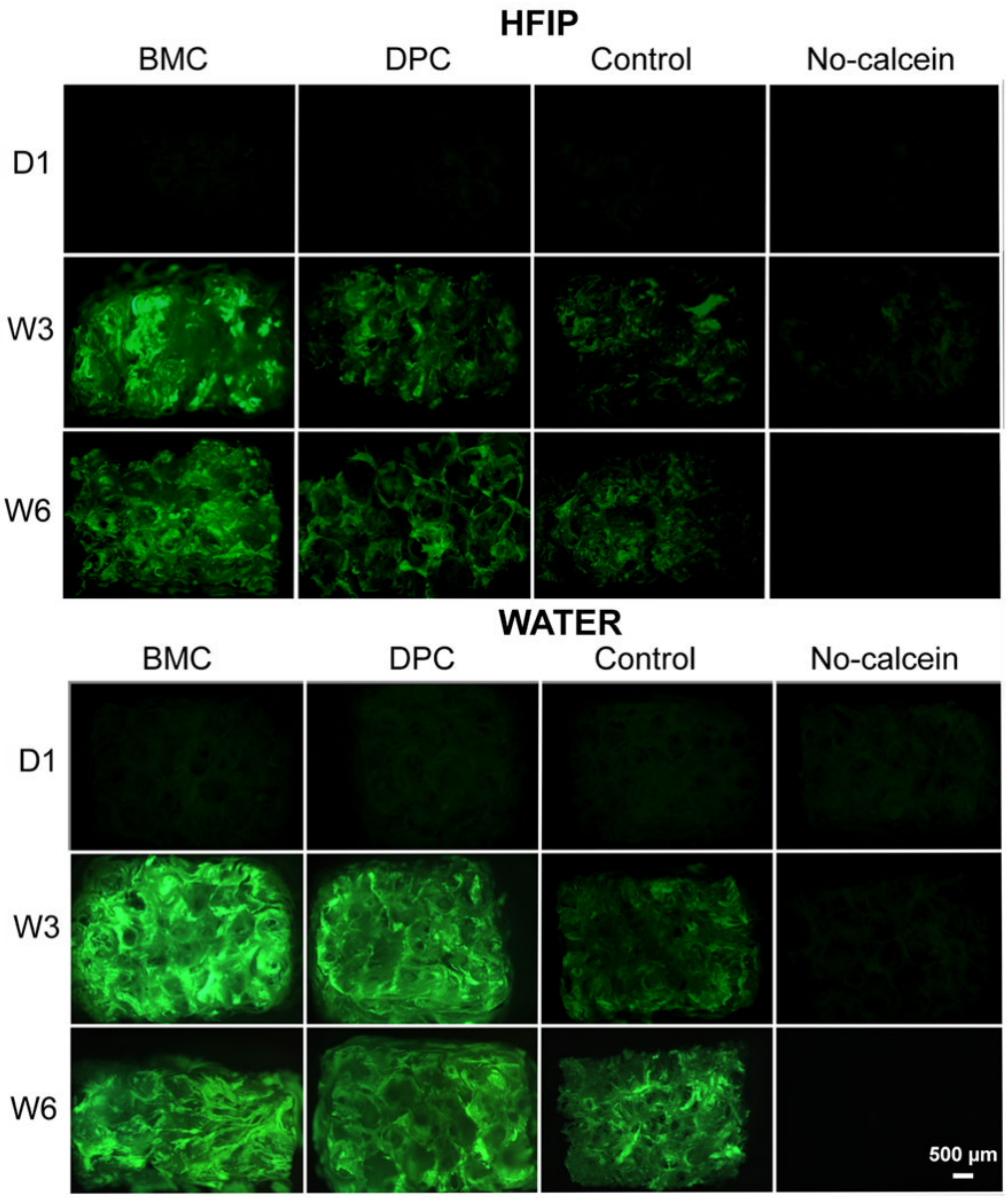

Figure 4. Calcein incorporation into in vitro cultured cell-seeded scaffold constructs

None of constructs cultured with Calcein appeared fluorescent after 1 day. In contrast, after three and six weeks of in vitro culture, distinct fluorescence due to Calcein incorporation were detected in all of the constructs, cultured with or without cells. No fluorescent signal was detected in scaffolds cultured in Calcein-free media.

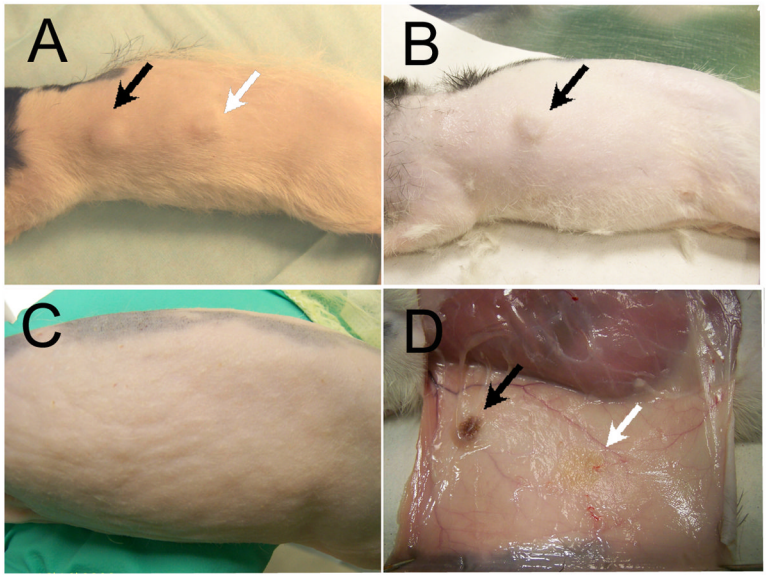

Figure 5. ***In vivo*** **human cell seeded-scaffold constructs implants**

A) After 6 weeks *in vivo* culture, immediately before harvesting. Both HFIP and water-based silk implants are noticeable under the skin. B) After 18 weeks *in vivo* culture, immediately before collection. Only HFIP based silk implants are noticeable. C) After 25 weeks *in vivo* culture, immediately before sample collection. None of the implants are detectable though the skin. D) When the skin is removed, HFIP based implants can be easily located, while aqueous based implants are quite degraded and difficult to find. Black arrows indicate HFIP based silk implant, and white arrow indicates aqueous based silk implant.

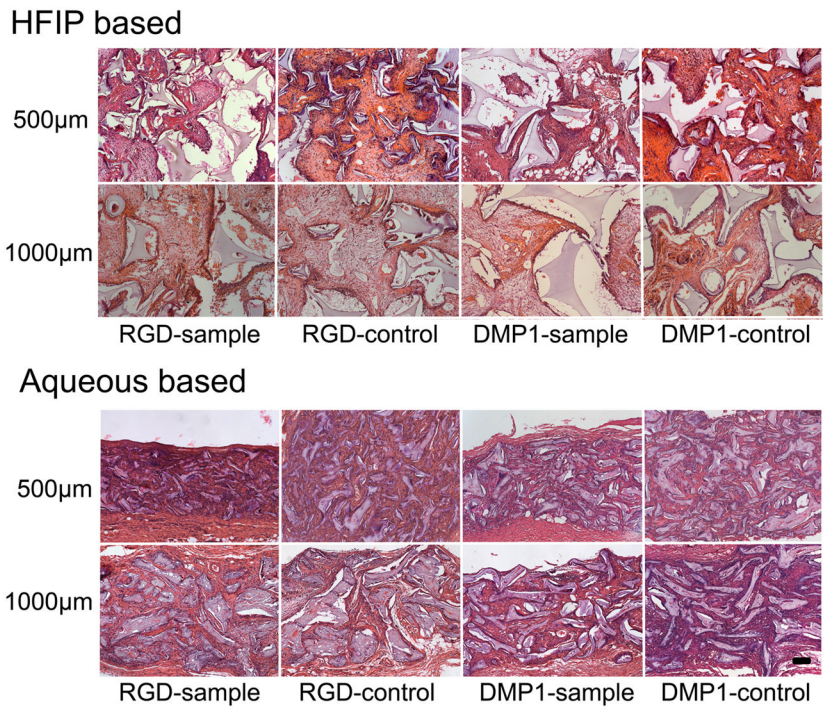

Figure 6. Sectioned *in vivo* cultured silk implants after 6 weeks implantation

Most HFIP based, and all water based silk scaffold pores appear to be filled with soft tissue. No hard tissues were detected. (Scale bar=100 μm).

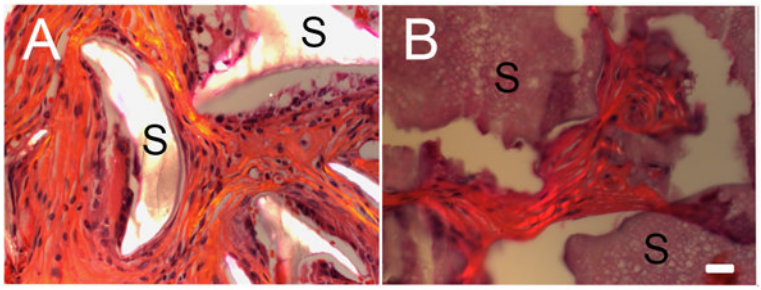

Figure 7. 25 week *in vivo* cultured silk implants. All photos were taken using polarized light microscopy

A) HFIP fabricated, 1000 μm pore sized silk scaffold coupled with RGD. Silk scaffold material is highlighted. Collagen ECM appears mature and well organized. B) Aqueous fabricated, 1000 μm pore sized silk scaffold coupled with RGD. Aqueous-fabricated silk scaffold material does not exhibit organized collagen fibers under polarized light microscopy. (Scale bar=20 μm)

Table 1

Silk degradation after 6 weeks *in vivo* culture.

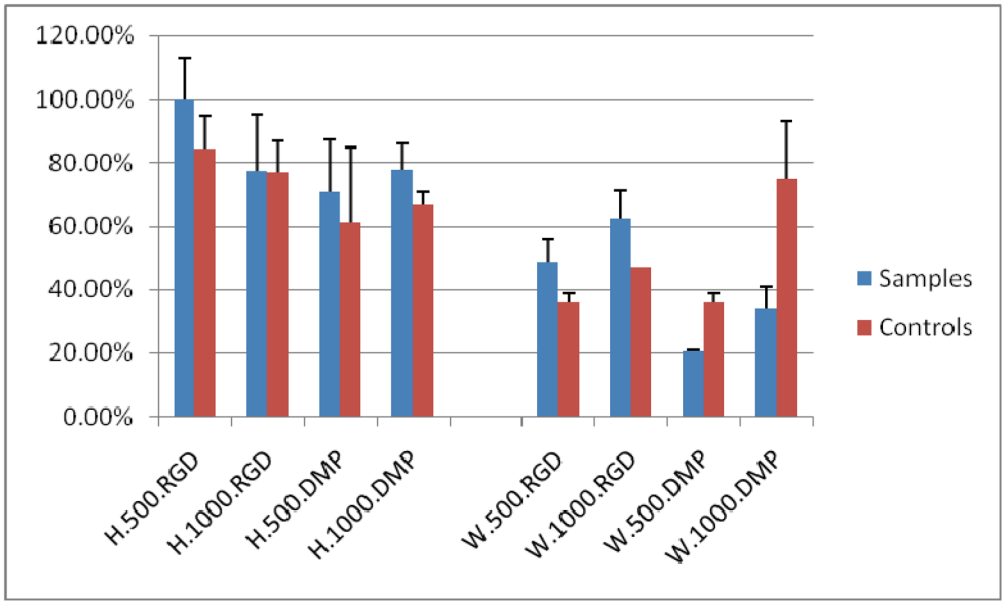

Table 2

Blood vessel formation in the implants after 6 weeks *in vivo* culture.